



# Stachel-independent modulation of GPR56/ADGRG1 signaling by synthetic ligands directed to its extracellular region

Gabriel S. Salzman<sup>a,b,c</sup>, Shu Zhang<sup>c</sup>, Ankit Gupta<sup>d</sup>, Akiko Koide<sup>d,e</sup>, Shohei Koide<sup>d,f,1</sup>, and Demet Araç<sup>c,g,1</sup>

<sup>a</sup>Biophysical Sciences Program, The University of Chicago, Chicago, IL 60637; <sup>b</sup>Medical Scientist Training Program, The University of Chicago, Chicago, IL 60637; <sup>c</sup>Department of Biochemistry and Molecular Biology, The University of Chicago, Chicago, IL 60637; <sup>d</sup>Perlmutter Cancer Center, New York University Langone Medical Center, New York, NY 10016; <sup>e</sup>Department of Medicine, New York University School of Medicine, New York, NY 10016; <sup>f</sup>Department of Biochemistry and Molecular Pharmacology, New York University School of Medicine, New York, NY 10016; and <sup>g</sup>Grossman Institute for Neuroscience, Quantitative Biology and Human Behavior, The University of Chicago, Chicago, IL 60637

Edited by Robert J. Lefkowitz, Howard Hughes Medical Institute, Duke University Medical Center, Durham, NC, and approved August 10, 2017 (received for review May 30, 2017)

**Adhesion G protein-coupled receptors (aGPCRs) play critical roles in diverse biological processes, including neurodevelopment and cancer progression. aGPCRs are characterized by large and diverse extracellular regions (ECRs) that are autoproteolytically cleaved from their membrane-embedded signaling domains. Although ECRs regulate receptor function, it is not clear whether ECRs play a direct regulatory role in G-protein signaling or simply serve as a protective cap for the activating “Stachel” sequence. Here, we present a mechanistic analysis of ECR-mediated regulation of GPR56/ADGRG1, an aGPCR with two domains [pentraxin and laminin/neurexin/sex hormonebinding globulin-like (PLL) and G protein-coupled receptor autoproteolysis-inducing (GAIN)] in its ECR. We generated a panel of high-affinity monoclonal antibodies directed to each of these domains, from which we identified activators and inhibitors of GPR56-mediated signaling. Surprisingly, these synthetic ligands modulated signaling of a GPR56 mutant defective in autoproteolysis and hence, in Stachel peptide exposure. These results provide compelling support for a ligand-induced and ECR-mediated mechanism that regulates aGPCR signaling in a transient and reversible manner, which occurs in addition to the Stachel-mediated activation.**

adhesion GPCR | allostery | cell signaling | monoclonal antibody | protein engineering

The G protein-coupled receptor (GPCR) superfamily exhibits great diversity with regard to the length and complexity of the extracellular region (ECR). Landmark mechanistic and functional studies of GPCRs to date have almost exclusively focused on receptors without prominent extracellular domains, particularly those from the rhodopsin family (1–3). In contrast, receptors from the adhesion, secretin, and frizzled/taste2 families and even some from the rhodopsin family have one or more extracellular domains (4). Members of the less well-studied adhesion G protein-coupled receptor (aGPCR) family are characterized by particularly diverse and large ECRs: hundreds to thousands of amino acid residues compose multiple protein domains (5, 6). Although their spatial proximity to the seven-pass transmembrane helices (7TM) region suggests potentially important roles for these complex ECRs in GPCR signaling (7), their functions are incompletely understood.

aGPCRs are expressed in many tissues and have been linked to myriad biological and physiological processes ranging from the establishment of ovarian cell polarity (Celsr1/ADGRC1) (8) to synapse formation (Lphn3/ADGRG3) (9) to regulation of lung surfactant production (GPR116/ARGRF5) (10). For example, the aGPCR GPR56/ADGRG1 is involved in cortex development, oligodendrocyte development, muscle cell development, innate immunity, and cancer progression (11–17). Recent studies have highlighted the role of GPR56 in promoting progression of acute myeloid leukemia (18) and progastrin-dependent colon cancer (19) and suggested that a GPR56 inhibitor would be clinically desirable.

A mechanistic understanding of the biology mediated by aGPCRs, and their ECRs in particular, will be a critical milestone on the path to treating aGPCR-mediated pathologies.

The aGPCR ECRs are characterized by the presence of a conserved juxtamembrane G protein-coupled receptor autoproteolysis-inducing (GAIN) domain (20) and various adhesion-type domains (located N-terminal to the GAIN domain), which allow aGPCRs to bind protein ligands (5, 21). An autoproteolytic event occurs within the GAIN domain during aGPCR maturation in the endoplasmic reticulum, cleaving the receptor into two fragments: an N-terminal fragment (NTF; composed of the N-terminal adhesion domains and the majority of the GAIN domain) and a C-terminal fragment (CTF; composed of the C-terminal  $\beta$ -strand of the GAIN domain termed “Stachel” or “stalk,” the 7TM, and the intracellular region) (Fig. 1). After cleavage, the NTF and CTF remain noncovalently but tightly associated throughout trafficking and localization to the plasma membrane (20, 22). The conservation of the GAIN domain suggests that it plays a role in aGPCR function. In this article, the term ECR represents all N-terminal adhesion domains as

## Significance

G protein-coupled receptors enable cells to sense extracellular signals and translate them into physiological responses. In addition to a transmembrane domain that transduces signals into the cytoplasm, adhesion G protein-coupled receptors (aGPCRs) have large extracellular regions (ECRs) that interact with proteins in the extracellular space. The goal of this study is to elucidate how ECRs control aGPCR activation. We engineered synthetic binding proteins, termed monoclonal antibodies, that bind specific domains in the ECR and showed that monoclonal antibodies can activate or inhibit G-protein signaling. Our data conclusively establish the feasibility of controlling aGPCR signaling using ECR-targeted drug-like molecules and support a model in which ligand binding to the ECR can affect the transmembrane domain and modulate signal transduction.

Author contributions: G.S.S., S.K., and D.A. designed research; G.S.S., S.Z., A.G., and D.A. performed research; G.S.S., A.K., S.K., and D.A. contributed new reagents/analytic tools; G.S.S., A.G., S.K., and D.A. analyzed data; and G.S.S., S.K., and D.A. wrote the paper.

Conflict of interest statement: A.K. and S.K. are listed as inventors on a patent filed by The University of Chicago that covers designs of monoclonal antibody libraries (US Patent 9512199 B2).

This article is a PNAS Direct Submission.

Freely available online through the PNAS open access option.

Data deposition: The DNA sequences of the monoclonal antibodies have been deposited in the GenBank nucleotide database with accession nos. MF668158–MF668176.

<sup>1</sup>To whom correspondence may be addressed. Email: Shohei.Koide@nyumc.org or arac@uchicago.edu.

This article contains supporting information online at [www.pnas.org/lookup/suppl/doi:10.1073/pnas.1708810114/-DCSupplemental](http://www.pnas.org/lookup/suppl/doi:10.1073/pnas.1708810114/-DCSupplemental).

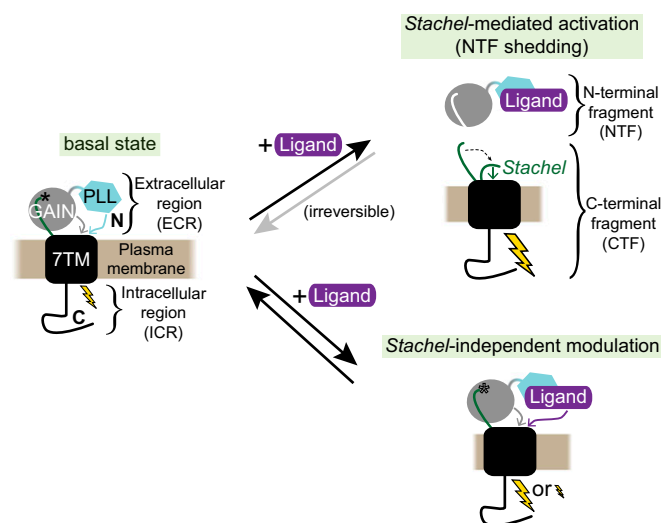


**Fig. 1.** Models for ligand-induced GPR56 G-protein signaling. Autoproteolysis site is indicated by an asterisk. Unneeded autoproteolysis indicated by an outlined asterisk. Lightning bolt size represents signaling intensity. Gray, cyan, and purple arrows represent proposed regulation of 7TM signaling by the ECR.

well as the entire GAIN domain, inclusive of the associated *Stachel* (compare ECR with NTF in Fig. 1).

Preliminary studies have proposed that GPCR ECRs regulate receptor functions, likely including G-protein signaling, on binding to extracellular ligands (9, 23–29). Two complementary models for ligand-induced aGPCR activation have been proposed (Fig. 1). In the *Stachel*-mediated model, the NTF serves as a protective cap for the *Stachel* and has no direct role in modulating 7TM function. On ligand binding to an N-terminal adhesion domain, the NTF dissociates from the CTF, termed “shedding,” exposing the *Stachel* to function as a “tethered agonist” (30–33). Key to this model is GAIN domain autoproteolysis, a necessary reaction to precede shedding and *Stachel* exposure. Although it has been proposed that natural ligands may induce shedding on binding to N-terminal adhesion domains and thereby, activate the receptor, direct proof of ligand-induced shedding remains elusive. Several recent observations, including that some aGPCRs do not undergo autoproteolysis and therefore, cannot undergo shedding (20, 34), have necessitated the introduction of a model, in which the ECR (i.e., associated NTF and *Stachel*) has a direct role in modulating the 7TM signaling (22, 33, 35, 36). Regulation by this mechanism, which we term “*Stachel*-independent,” is independent of *Stachel*-mediated activation, although the *Stachel* residues are present within the core of the GAIN domain (Fig. 1). In this model, the ECR directly communicates with the 7TM (i.e., via transient interactions), such that ligand binding events or conformational changes in the ECR may directly result in altered signaling. Direct proof of this model has also remained elusive. A major bottleneck in discriminating these mechanisms is a lack of high-affinity, water-soluble ligands that can perturb aGPCR function in a well-controlled manner. Although natural ligands have been identified for several aGPCRs (5), many of them are not suitable for quantitative assays.

GPR56 is among the better characterized members of the aGPCR family. It has a 377-residue ECR composed of two domains: an N-terminal pentraxin and laminin/neurexin/sex hormone-binding globulin-like (PLL) domain and a GAIN domain (36). Previously, we have shown that deletion of the PLL domain increases basal activity of the receptor (36). Additionally, we engineered a binding protein, termed monobody  $\alpha 5$ , that targets the ECR of mouse GPR56, bridges the PLL and GAIN domains, and functions as an allosteric inverse agonist of G-protein signaling.

Although both of these findings support ECR-mediated regulation of signaling, mechanistic detail was lacking.

In this study, we set out to elucidate the regulatory mechanism of aGPCR signaling by ligands to the ECR. To this end, we developed a panel of monobodies that target specific extracellular domains of human (h) and mouse (m) GPR56 and identified an activator and an inhibitor of human GPR56 among these monobodies. Based on the activity of these synthetic ligands on an autoproteolysis-defective and thus, shedding-defective receptor, our results provide support for *Stachel*-independent regulation of GPR56 signaling mediated by the ECR.

## Results

**Monobodies Targeted to GAIN and PLL Domains of Mouse and Human GPR56.** Guided by the knowledge of the structure of the ECR and the autoinhibitory role of the PLL domain gained from our previous work (36), we hypothesized that ligands that engaged different regions within the ECR would differentially affect GPR56 signaling. In addition, we were interested in developing a detection reagent for splice variant 4 (S4), which has an ECR that is composed of only the GAIN domain as a consequence of alternative splicing leading to deletion of the N-terminal 175 residues (including the signal peptide, PLL domain, and PLL–GAIN linker) (Fig. S1A). As we have shown that PLL domain deletion results in increased basal activity (36), we were particularly interested in facilitating the study of S4 expression and function. Taken together, we set out to engineer a diverse panel of monobodies for the ECRs of human and mouse GPR56.

Because the ECRs of mouse and human GPR56 are not highly conserved (73% amino acid sequence identity), we anticipated that most monobodies would not cross-react with both human and mouse GPR56. Indeed, this was the case for the  $\alpha 5$  monobody that we generated previously (36). Consequently, we decided to perform monobody selection separately for human and mouse GPR56 samples. We prepared the purified samples of the full-length ECRs as well as individual PLL and GAIN domains of both mouse and human GPR56. Although the single-domain constructs have exposed hydrophobic surfaces that would be sequestered in the interface between the PLL and GAIN domains, they were highly soluble and predominantly monomeric. Using a total of six samples as antigens, we carried out phage and yeast display selection of monobodies as previously described (36, 37) and identified 19 clones (Table S1). These included human GPR56-specific clones that bind to the PLL domain but not the GAIN domain [e.g., Mb(hGPR56\_ $\beta 7$ )], to the GAIN domain but not the PLL domain [e.g., Mb(hGPR56\_ $\beta 6$ )], and to full-length ECR but not the PLL or GAIN domain in isolation [e.g., Mb(hGPR56\_ $\beta 1$ )] (Fig. 2A). We obtained similar clones specific to mouse GPR56 (Fig. 2A and Table S2). Surprisingly, we also identified monobodies that bind the human and mouse GAIN domains [e.g., Mb(hGPR56\_ $\beta 3$ )] (Fig. 2A and B), although our selection strategy was not designed to enrich such cross-reactive clones. Four particularly interesting clones will be the focus hereafter: Mb(hGPR56\_ $\beta 1$ ), Mb(hGPR56\_ $\beta 3$ ), Mb(hGPR56\_ $\beta 7$ ), and Mb(mGPR56\_ $\beta 12$ ), hereafter abbreviated  $\beta 1$ ,  $\beta 3$ ,  $\beta 7$ , and  $\beta 12$ , respectively. Their properties are summarized in Fig. 2, Fig. S2, and Tables S2 and S3.

Given our interest in facilitating S4 characterization, we set out to test if a GAIN domain-specific monobody,  $\beta 3$ , could detect S4 on the cell surface. To this end, we expressed a  $\Delta$ PLL mouse GPR56 construct, equivalent to the predicted protein product of S4, in HEK293T cells (36) and costained cells with  $\alpha 5$  and  $\beta 3$ . We measured a robust increase in  $\beta 3$  binding signal for both WT and  $\Delta$ PLL GPR56 compared with empty vector, strongly suggesting that  $\beta 3$  detects the predicted protein product of S4 (Fig. S1B). As there are no other reagents, to our knowledge, that specifically detect the truncated ECR of S4,  $\beta 3$  may prove useful in future studies of S4 expression.

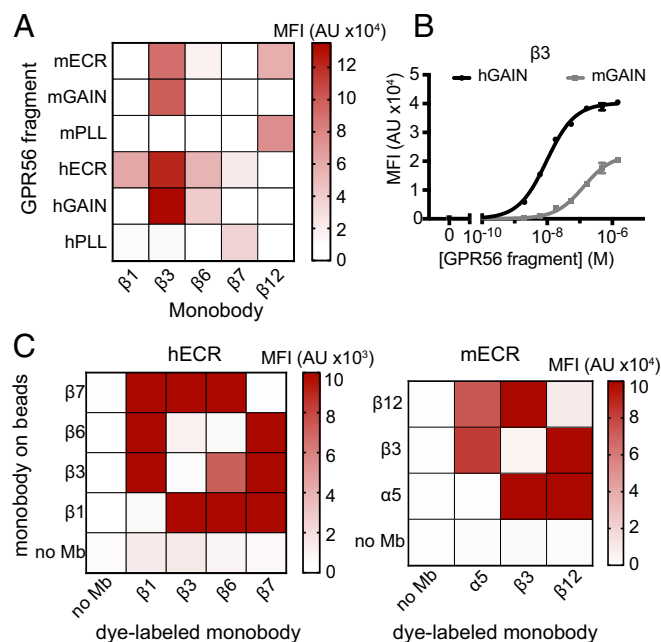


**Fig. 2.** Characterization of domain-specific GPR56-binding monobodies. (A) Purified human and mouse GPR56 fragments (1.1  $\mu$ M) binding to monobody-coated M280 beads. ECR fragment consists of PLL domain + PLL-GAIN linker + GAIN domain. (B) Yeast-displayed  $\beta$ 3 binding to GPR56 GAIN domains.  $K_d$  values were determined for human and mouse GAIN domains to be  $9.6 \pm 0.6$  and  $130 \pm 15$  nM, respectively. Error bars indicated SEM ( $n = 3$ ). (C) “Sandwich” format binding assay, whereby purified monobodies from the vertical axis were immobilized on M280 beads and incubated first with unlabeled human (Left) or mouse (Right) GPR56 ECR followed by staining with purified monobodies from the horizontal axis, which were detected with fluorescently labeled neutravidin. By design, any protein pairs that bind overlapping sites on the ECR of GPR56 result in low binding signal. Conversely, protein pairs with nonoverlapping binding sites on GPR56 yield high binding signal. Mb, monobody; MFI, median fluorescence intensity.

**Monobodies Modulate G Protein Signaling.** We examined whether the monobodies affect activity of GPR56 using a serum response element (SRE)-luciferase assay that measures signaling via  $G\alpha_{13}$  (32, 36) (Fig. 3A and B). Monobody  $\beta$ 1 decreased hGPR56 signaling (Fig. 3A). In contrast,  $\beta$ 1 treatment of mGPR56- or empty vector-transfected cells resulted in no detectable change in signaling, showing its specificity for human GPR56 (Fig. 3A and B).  $\beta$ 1 decreased hGPR56 signaling with  $IC_{50}$  of  $70 \pm 30$  nM, resulting in a  $\sim 1.6$ -fold decrease in signaling relative to the basal activity (Fig. 3C). Notably,  $\beta$ 1 had a profile similar to  $\alpha$ 5, a previously reported monobody directed to mouse GPR56, in that both bound the full ECR but not the isolated GAIN or PLL domain, and functioned as an allosteric inverse agonist of G-protein signaling (36, 38).

In contrast to  $\beta$ 1,  $\beta$ 7 that targeted the PLL domain increased signaling of hGPR56 with  $EC_{50}$  of  $800 \pm 500$  nM, resulting in a  $\sim 1.6$ -fold increase in signaling relative to basal activity (Fig. 3C), and thus, may be classified as an allosteric agonist of G-protein signaling (38). The effect of  $\beta$ 7 was also specific to human GPR56 (Fig. 3A and B). This stimulatory monobody of GPR56 is characterized here.

Monobody  $\beta$ 3 that bound the GAIN domain of both human and mouse GPR56 exhibited no significant effect on signaling in this assay. Although the binding profiles in Fig. 2A indicate that the epitopes for both  $\beta$ 1 and  $\beta$ 3 include the GAIN domain, the two epitopes do not overlap (Fig. 2C). This observation suggests that these two monobodies engaged the GAIN domain in distinct manners.

**Activating and Inhibiting Monobodies Modulate Signaling of an Autoproteolysis-Defective GPR56 Mutant.** We next set out to determine whether these synthetic GPR56 ligands functioned in a *Stachel*-mediated or *Stachel*-independent manner. To this end, we introduced a single-point mutation, H381S, in the GAIN domain of human and mouse GPR56 previously shown to abolish GAIN domain-mediated autoproteolysis and therefore, *Stachel*-exposure without affecting the overall structure of the ECR (20, 33, 36). In this study, we confirmed that WT GPR56 underwent near-complete autoproteolysis, which the H381S mutation abolished (Fig. S3A). Furthermore, monobody treatment had no significant effect on autoproteolysis or shedding in cell culture (Fig. S3B). We compared the effect of monobody treatment on G-protein signaling of WT and H381S mutant GPR56 using the SRE-luciferase assay (Fig. 4). The effects of  $\alpha$ 5,  $\beta$ 1, and  $\beta$ 7 were essentially indistinguishable for both receptors (Fig. 4D), showing that their effects on G-protein signaling measured in this assay are independent of autoproteolysis. Finally, to test if the monobodies functioned in an autoproteolysis-independent but *Stachel*-dependent manner, we mutated a highly conserved *Stachel* residue, F385, previously shown to be critical for *Stachel*-mediated activation of several aGPCRs, including GPR56 (30, 32). The F385A mutation did not abolish monobody-mediated modulation of GPR56 signaling (Fig. S4). Thus, we conclude that neither autoproteolysis nor *Stachel*-mediated activation are required for the monobody-mediated modulation of GPR56 signaling.

## Discussion

**Synthetic GPR56 Ligands Elucidate Direct Regulation of Signaling by the ECR.** In this study, we set out to engineer synthetic protein ligands targeted to the ECR of human GPR56 and obtained an allosteric agonist ( $\beta$ 7) and an allosteric inverse agonist ( $\beta$ 1) (Figs. 1–3). Thus, we have substantially expanded the available tools for modulating WT human GPR56 signaling by targeting its ECR. Along with the previously characterized allosteric inverse agonist, the  $\alpha$ 5 monobody (36), we show that autoproteolysis is not required for each of these functional monobodies to modulate signaling (Fig. 4). These results strongly suggest that perturbations to the ECR are directly sensed by the 7TM, resulting in altered signaling without NTF shedding and *Stachel* exposure (Fig. 5).

Binding characteristics of the monobodies give additional insights into the molecular mechanism of GPR56 regulation. The allosteric inverse agonists,  $\alpha$ 5 and  $\beta$ 1, bound to the full-length ECR but not to the isolated GAIN or PLL domain (36) (Fig. 2). The X-ray crystal structure of the  $\alpha$ 5-ECR complex revealed that  $\alpha$ 5 interacts with both the PLL and GAIN domains (36), leading to the speculation that  $\alpha$ 5 and probably  $\beta$ 1 decrease basal activity by restricting the interdomain motions of the ECR. Unlike these inverse agonists,  $\beta$ 7, the allosteric agonist, binds more tightly to the PLL domain alone than it does for the full ECR (Fig. 2A and Table S3), indicating that it binds to a region of the PLL domain that is less accessible in the full ECR, probably blocked by the GAIN domain or PLL-GAIN linker. As such, we speculate that, by binding to the PLL domain within the full ECR,  $\beta$ 7 disrupts the PLL-GAIN interface, thereby inducing a conformational change in the ECR or altering transient interactions between the ECR and 7TM and leading to increased basal activity of the WT receptor. Taken together, the distinct binding profiles of agonist and inverse agonist monobodies suggest that alterations of the relative orientation between the GAIN and PLL domains contribute to regulation of GPR56 signaling. Alternatively, these results also suggest the possibility in which ECR-bound monobodies directly interact with the 7TM and modulate signaling. Future studies will determine the contributions of these complementary mechanisms.

The location of the *Stachel* sequence within the GAIN domain strongly suggests that NTF shedding is autoproteolysis-dependent and irreversible. In the 3D structure, the hydrophobic *Stachel* is buried within the hydrophobic core of the GAIN domain and forms

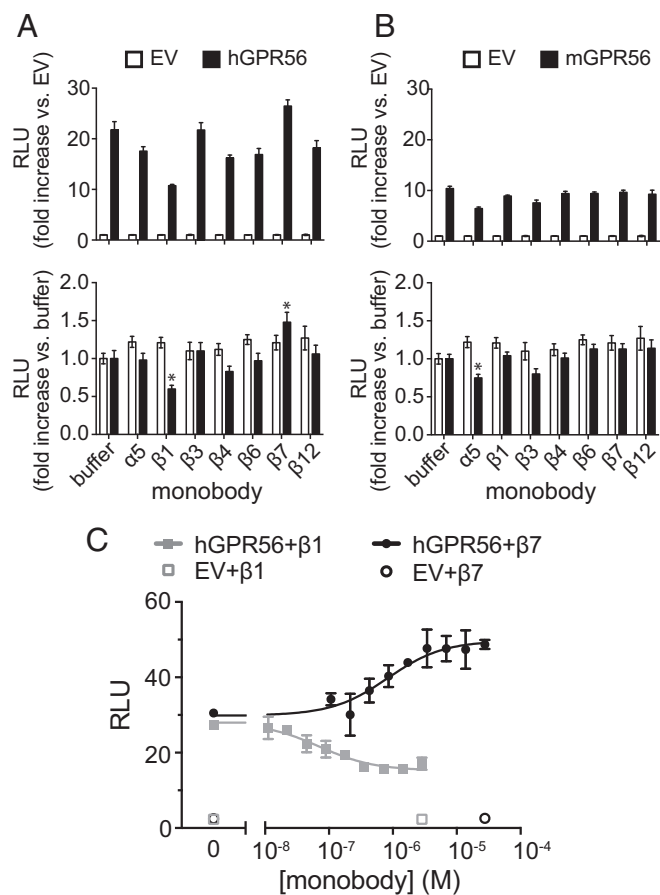


**Fig. 3.** Modulation of WT GPR56 signaling by monobodies. (A and B) SRE-luciferase assay for G-protein signaling of (A) human and (B) mouse GPR56 in the presence of 0.7  $\mu$ M purified monobodies presented as fold increase vs. empty vector (EV) (Upper) and fold increase vs. buffer (Lower). Significant effects are representative of many repeated experiments. RU, response unit. \* $P < 0.05$  vs. buffer treatment by Student's two-tailed  $t$  test. (C) Titration of monobodies  $\beta 1$  and  $\beta 7$  on SRE-luciferase activity of WT human GPR56. The  $IC_{50}$  value of  $\beta 1$  was determined to be  $70 \pm 30$  nM. The  $EC_{50}$  value of  $\beta 7$  was determined to be  $800 \pm 500$  nM. Error bars indicated SEM ( $n = 3$ ).

extensive hydrogen bond networks with adjacent  $\beta$ -strands (20, 36). This architecture strongly suggests that exposure of the *Stachel* requires substantial deformation of the GAIN domain. Furthermore, because the *Stachel* is a central part of the GAIN domain, the release of the *Stachel* from the GAIN domain most likely leads to a collapse of the original conformation, prohibiting reassociation of the *Stachel* with the NTF. Although the N-terminal residues of the *Stachel* are the most deeply buried within the GAIN domain (20, 36), they are critical for mediating receptor activation (30, 32). Thus, transient exposure of the *Stachel* to activate the 7TM without causing irreversible NTF-CTF dissociation should be an extremely rare event, if not practically impossible. Therefore, we propose that (i) autoproteolysis is a necessary prerequisite for *Stachel*-mediated aGPCR activation and that (ii) the process of *Stachel* exposure is irreversible.

Our observations that the WT receptor as well as the autoproteolysis-defective and *Stachel*-defective mutants were all susceptible to monobody-mediated modulation (Fig. 4 and Fig. S4) represent among the most concrete evidence to date that aGPCR signaling can be regulated in an autoproteolysis- and *Stachel*-independent manner. The inhibitory efficacy of  $\beta 1$  is consistent for the WT, H381S, F385A, and H381S + F385A constructs (Fig. S4). Similarly,  $\beta 7$ -mediated modulation was observed in the absence of autoproteolysis and/or *Stachel*-mediated

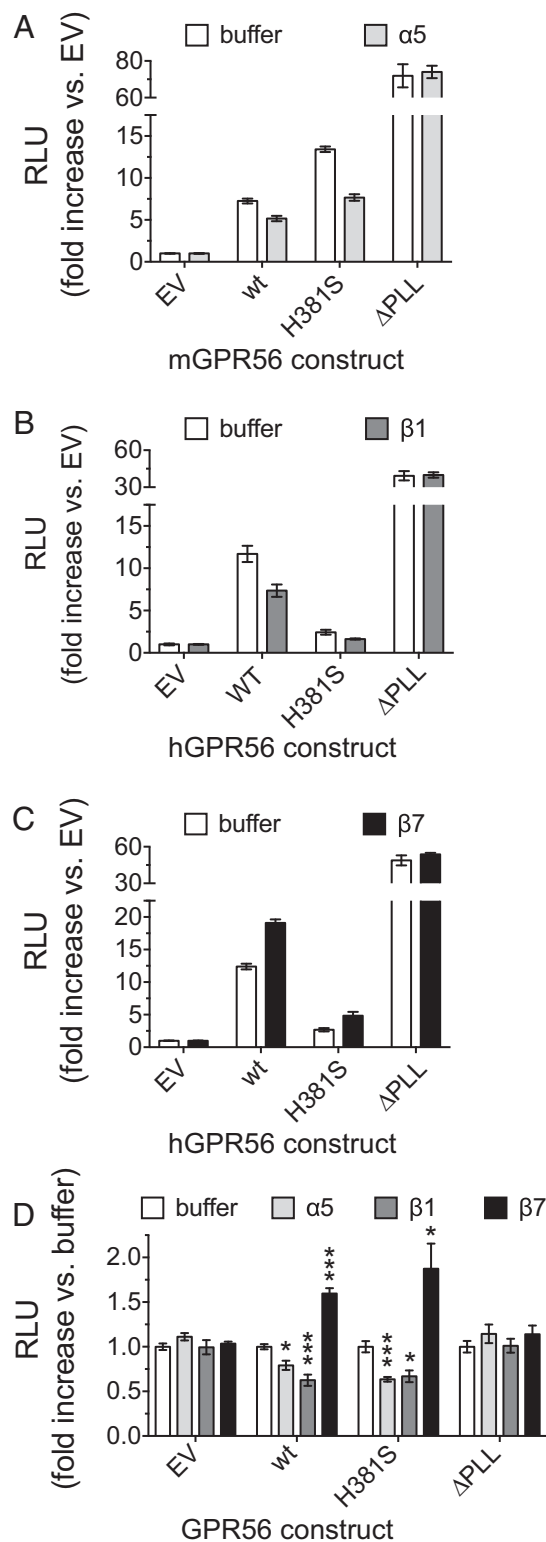


**Fig. 4.** Monobody-mediated activation and inhibition of GPR56 is autoproteolysis-independent. SRE-luciferase assay of indicated GPR56 constructs in the presence of buffer or monobody. (A) Mouse GPR56 constructs treated with 4.9  $\mu$ M  $\alpha 5$ . (B and C) Human GPR56 constructs treated with (B) 2.9  $\mu$ M  $\beta 1$  and (C) 27.5  $\mu$ M  $\beta 7$ . (D) Data from A–C normalized to buffer treatment to account for differences in measured basal activity of GPR56 constructs, which we have previously shown is, in part, because of differences in cell surface expression (36). Error bars indicated SEM ( $n = 3$ ). \* $P < 0.05$  vs. buffer treatment by Student's two-tailed  $t$  test; \*\*\* $P < 0.001$  vs. buffer treatment by Student's two-tailed  $t$  test. EV, empty vector.

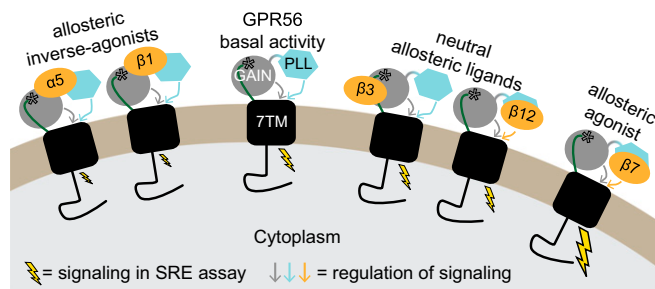


**Fig. 5.** Proposed mechanisms for distinct monobody-dependent modulation of GPR56 function. Monobodies are arranged based on function, and GPR56 domains necessary for binding are illustrated. Lightning bolt size represents signaling intensity. Autoprolysis site indicated by an asterisk. Unneeded autoprolysis indicated by outlined asterisks. Rather than direct interactions, colored arrows represent regulation of 7TM signaling by the ECR or monobodies. Designations of “allosteric inverse agonist,” “neutral allosteric ligand,” and “allosteric agonist” are based on definitions proposed by Christopoulos et al. (38).

activation (Fig. S4), although its effects for these constructs varied, suggesting an additional level of complexity to be uncovered. Together, our results strongly support the presence of *Stachel*-independent modes of aGPCR signaling.

**A Unified Model of Ligand-Mediated Regulation of aGPCRs.** The biological relevance of *Stachel*-mediated aGPCR activation is extremely clear (23, 25, 30–32, 39, 40). However, unanswered questions and recent observations have necessitated the introduction of the complementary *Stachel*-independent model (33). For example, overexpression of autoprolysis-deficient *lat-1/ADGRL1* in *lat-1-KO Caenorhabditis elegans* rescues the WT phenotype, suggesting that some aGPCR functions do not require autoprolysis (41). Additionally, there are several aGPCRs that lack the conserved residues critical for autoprolysis and therefore, remain uncleaved (20, 34). Furthermore, several aGPCRs, including GPR56, are found partially uncleaved in vivo (20, 36, 42). For example, GPR56 in skeletal muscle was found to be almost completely uncleaved (42), although it plays critical roles in skeletal muscle cells (11, 43). Together, these observations suggest that *Stachel*-independent mechanisms may play important roles in aGPCR signaling.

Our key observation that ECR ligands modulate signaling in an autoprolysis-independent manner complements the recent studies by Kishore et al. (33) and Kishore and Hall (44), in which they measured the basal activities of GPR56 constructs with various ECR truncations through multiple signaling pathways. Using an SRE-luciferase assay, a construct lacking the NTF (i.e., 7TM with exposed *Stachel*) (Fig. 1) had the highest activity, whereas one lacking both the NTF and the *Stachel* (i.e., just the 7TM) had the lowest activity (33), confirming the agonistic function of *Stachel* on the 7TM (32). In comparison, the full-length constructs of both the WT and an autoprolysis-deficient mutant exhibited a moderate level of activity (33), suggesting that the ECR modulates 7TM signaling.

In contrast to the *Stachel*-mediated activation, ECR-mediated *Stachel*-independent regulation is likely to be moderate and require no receptor turnover for resetting the signal, because ECR ligands interact with aGPCRs in a reversible manner. Thus, the *Stachel*-independent regulation should be suited for fine-tuning the signaling near the basal levels. The value of this mechanistic insight is clear from a pharmacological point of view, as the therapeutic benefits of inducing moderate and enormous changes, usually with allosteric and orthosteric ligands, respectively, in GPCR signaling have both been repeatedly shown (45–49).

In addition to the mechanistic insight gleaned from these monobodies, the recent discovery of several synthetic small

molecule ligands of GPR56 has furthered the potential for development of aGPCR-targeted therapeutics in the near future (50). The powerful combination of ECR-targeted synthetic proteins, including monobodies and antibodies (35, 40, 51), with 7TM-targeted small molecule ligands will be invaluable in future mechanistic and pharmacological studies of aGPCRs.

## Experimental Procedures

**Cloning and Purification of GPR56 Extracellular Domains from Insect Cells.** The following constructs were prepared and cloned into pAcGP67a for expression in insect cells: human GPR56 (Q9Y653; UniProt) full ECR (residues G27–S392), PLL domain (residues G27–S160), and GAIN domain (residues M176–S392) and mouse GPR56 (Q8K209; UniProt) full ECR (residues S27–S392), PLL domain (residues G27–S160), and GAIN domain (residues M176–S392). The C121S and C177S mutations were introduced to the PLL and GAIN domain constructs, respectively, to remove the free cysteine residues that participate in the interdomain disulfide bond in the full ECR (36). A C-terminal His<sub>6</sub> tag was added for affinity purification. A C-terminal biotin ligase recognition sequence (AVI tag) corresponding to the sequence GLNDIFEAQKIEWHE was added to aid biotinylation.

A baculovirus expression system was used for expression of proteins in High Five insect cells as previously described (20). The secreted, glycosylated proteins were purified using nickel-nitrilotriacetic agarose resin (Qiagen) and size-exclusion chromatography (Superdex 200 10/300 GL; GE Healthcare).

**Monobody Generation.** Purified and biotinylated human and mouse full ECR, GAIN domain, and PLL domain were used as targets for phage display selection from a “side and loop” monobody library as previously described (37). The naive phage display library contained  $\sim 10^9$  different clones (37). Three rounds of selection were performed at target concentrations of (i) 100 nM (conjugated to streptavidin beads and thus, in the tetravalent form), (ii) 100 nM (monomeric), and (iii) 50 nM (monomeric). In some cases, the species was altered for the second round of selection in an attempt to generate human and mouse cross-reactive clones. A yeast display library containing  $\sim 10^6$  different clones was constructed from the output of phage display selection. Two rounds of positive sorting of the yeast display library were done using fluorescence-activated cell sorting using the same GPR56 domains labeled with dye to stain yeast. Binding assays testing the affinity and specificity of individual monobody clones were performed using yeast surface display and M280 beads as described previously (36, 52).

**Purification of Monobodies from *Escherichia coli*.** The genes encoding the identified monobodies were cloned into an expression vector, pHBT (52). Monobodies were expressed in BL21(DE3) *E. coli* via isopropyl  $\beta$ -D-1-thiogalactopyranoside (IPTG) induction at 18 °C for 20 h. Monobodies were purified via an N-terminal 6xHIS tag using nickel-nitrilotriacetic agarose resin (Qiagen);  $\beta$ 3 was refolded on the Ni column using the  $\beta$ -cyclodextrin method (53),  $\beta$ 1 and  $\beta$ 7 were refolded in solution using the L-Arginine dilution method (54), and  $\beta$ 12 was purified from the soluble fraction of *E. coli* lysate without refolding. Proteins were further purified using a Superdex 200 10/300 GL column (GE Healthcare).

**SRE-Luciferase Signaling Assay.** SRE-luciferase assay was performed as described previously (36) with several alterations. Briefly, HEK293T cells were seeded in 96-well plates (10,000 cells in 0.1 mL DMEM + 10% FBS per well). After 12–18 h, cells reached 40–50% confluence and were transfected with 10 ng *GPR56/Gpr56* (WT or mutant) + 20 ng dualLuc-SRE + 0.3  $\mu$ L LipoD293 (SigmaGen) per well from a master mix. After 24 h, media were aspirated and replaced with DMEM without FBS. For monobody treatment, monobody was added to cells 6.5 h after the start of serum starvation. After 12 h total of serum starvation, media were aspirated. Cells were lysed using the Dual-Glo Luciferase Assay System from Promega, and firefly and renilla luciferase signals were measured using a Synergy HTX luminescence plate reader. Signaling intensity in relative luminescence units (RLU) (fold increase) is reported as  $(\text{Firefly}_{\text{GPR56}}/\text{Renilla}_{\text{GPR56}})/(\text{Firefly}_{\text{EV}}/\text{Renilla}_{\text{EV}})$ .

**Flow Cytometry.** HEK293T cells were transiently transfected with WT or mutant mouse *GPR56* constructs using LipoD293. After 48 h, cells were detached with citric saline and costained with blocked  $\beta$ 3-neutravidin-DyLight488 precomplex and blocked  $\alpha$ 5-neutravidin-DyLight650 precomplex in a single 20-min staining reaction in PBS + 2% bovine serum albumin at room temperature. Flow cytometry was performed using Accuri C6 flow cytometer.

**Resource Sharing Plan.** All monobody sequences are available in Table S1. Other reagents can be obtained from the corresponding authors under a material transfer agreement.

**ACKNOWLEDGMENTS.** We thank Engin Özkan for use of his flow cytometer and Chuan He for use of his luminescence plate reader. Celia Fernandez contributed to an optimized SRE-luciferase assay protocol. This work was

supported by NIH Grants F30-GM116455 (to G.S.S.), U54-GM087519 (to S.K.), R01-GM120322 (to D.A.), and T32GM007183; Brain Research Foundation (D.A.); and Big Ideas Generator (D.A.).

1. Rasmussen SGF, et al. (2011) Crystal structure of the  $\beta 2$  adrenergic receptor-Gs protein complex. *Nature* 477:549–555.
2. Hoffman BB, Lefkowitz RJ (1982) Adrenergic receptors in the heart. *Annu Rev Physiol* 44:475–484.
3. Samama P, Pei G, Costa T, Cotecchia S, Lefkowitz RJ (1994) Negative antagonists promote an inactive conformation of the beta 2-adrenergic receptor. *Mol Pharmacol* 45:390–394.
4. Fredriksson R, Lagerström MC, Lundin LG, Schiöth HB (2003) The G-protein-coupled receptors in the human genome form five main families. Phylogenetic analysis, paralogue groups, and fingerprints. *Mol Pharmacol* 63:1256–1272.
5. Langenhan T, Aust G, Hamann J (2013) Sticky signaling—Adhesion class G protein-coupled receptors take the stage. *Sci Signal* 6:re3.
6. Paavola KJ, Hall RA (2012) Adhesion G protein-coupled receptors: Signaling, pharmacology, and mechanisms of activation. *Mol Pharmacol* 82:777–783.
7. Yang L, et al. (2015) Conformational states of the full-length glucagon receptor. *Nat Commun* 6:7859.
8. Shi D, et al. (2014) Celsr1 is required for the generation of polarity at multiple levels of the mouse oviduct. *Development* 141:4558–4568.
9. O'Sullivan ML, et al. (2012) FLRT proteins are endogenous latrophilin ligands and regulate excitatory synapse development. *Neuron* 73:903–910.
10. Fukuzawa T, et al. (2013) Lung surfactant levels are regulated by Ig-Hepta/GPR116 by monitoring surfactant protein D. *PLoS One* 8:e69451.
11. White JP, et al. (2014) G protein-coupled receptor 56 regulates mechanical overload-induced muscle hypertrophy. *Proc Natl Acad Sci USA* 111:15756–15761.
12. Piao X, et al. (2004) G protein-coupled receptor-dependent development of human frontal cortex. *Science* 303:2033–2036.
13. Giera S, et al. (2015) The adhesion G protein-coupled receptor GPR56 is a cell-autonomous regulator of oligodendrocyte development. *Nat Commun* 6:6121.
14. Ackerman SD, Garcia C, Piao X, Gutmann DH, Monk KR (2015) The adhesion GPCR GPR56 regulates oligodendrocyte development via interactions with  $\alpha 12/13$  and RhoA. *Nat Commun* 6:6122.
15. Chang G-W, et al. (2016) The adhesion G protein-coupled receptor GPR56/ADGRG1 is an inhibitory receptor on human NK cells. *Cell Rep* 15:1757–1770.
16. Saito Y, et al. (2013) Maintenance of the hematopoietic stem cell pool in bone marrow niches by EVI1-regulated GPR56. *Leukemia* 27:1637–1649.
17. Yang L, Friedland S, Corson N, Xu L (2014) GPR56 inhibits melanoma growth by internalizing and degrading its ligand TG2. *Cancer Res* 74:1022–1031.
18. Pabst C, et al. (2016) GPR56 identifies primary human acute myeloid leukemia cells with high repopulating potential in vivo. *Blood* 127:2018–2027.
19. Jin G, et al. (2017) The G-protein coupled receptor 56, expressed in colonic stem and cancer cells, binds progastrin to promote proliferation and carcinogenesis. *Oncotarget* 8:40606–40619.
20. Araç D, et al. (2012) A novel evolutionarily conserved domain of cell-adhesion GPCRs mediates autoprolysis. *EMBO J* 31:1364–1378.
21. Lu YC, et al. (2015) Structural basis of latrophilin-FLRT-UNC5 interaction in cell adhesion. *Structure* 23:1678–1691.
22. Paavola KJ, Stephenson JR, Ritter SL, Alter SP, Hall RA (2011) The N terminus of the adhesion G protein-coupled receptor GPR56 controls receptor signaling activity. *J Biol Chem* 286:28914–28921.
23. Luo R, et al. (2014) Mechanism for adhesion G protein-coupled receptor GPR56-mediated RhoA activation induced by collagen III stimulation. *PLoS One* 9:e100043.
24. Chiang N-Y, et al. (2016) Heparin interacts with the adhesion GPCR GPR56, reduces receptor shedding, and promotes cell adhesion and motility. *J Cell Sci* 129:2156–2169.
25. Petersen SC, et al. (2015) The adhesion GPCR GPR126 has distinct, domain-dependent functions in Schwann cell development mediated by interaction with laminin-211. *Neuron* 85:755–769.
26. Coin I, et al. (2013) Genetically encoded chemical probes in cells reveal the binding path of urocortin-I to CRF class B GPCR. *Cell* 155:1258–1269.
27. Byrne EFX, et al. (2016) Structural basis of smoothened regulation by its extracellular domains. *Nature* 535:517–522.
28. Zhao L-H, et al. (2016) Differential requirement of the extracellular domain in activation of Class B G protein-coupled receptors. *J Biol Chem* 291:15119–15130.
29. Booe JM, et al. (2015) Structural basis for receptor activity-modifying protein-dependent selective peptide recognition by a G protein-coupled receptor. *Mol Cell* 58:1040–1052.
30. Liebscher I, et al. (2014) A tethered agonist within the ectodomain activates the adhesion G protein-coupled receptors GPR126 and GPR133. *Cell Rep* 9:2018–2026.
31. Demberg LM, Rothmund S, Schöneberg T, Liebscher I (2015) Identification of the tethered peptide agonist of the adhesion G protein-coupled receptor GPR64/ADGRG2. *Biochem Biophys Res Commun* 464:743–747.
32. Stoveken HM, Hajduczuk AG, Xu L, Tall GG (2015) Adhesion G protein-coupled receptors are activated by exposure of a cryptic tethered agonist. *Proc Natl Acad Sci USA* 112:6194–6199.
33. Kishore A, Purcell RH, Nassiri-Toosi Z, Hall RA (2016) Stalk-dependent and stalk-independent signaling by the adhesion G protein-coupled receptors GPR56 (ADGRG1) and BAI1 (ADGRB1). *J Biol Chem* 291:3385–3394.
34. Prömel S, et al. (2012) Characterization and functional study of a cluster of four highly conserved orphan adhesion-GPCR in mouse. *Dev Dyn* 241:1591–1602.
35. Ohta S, et al. (2015) Agonistic antibodies reveal the function of GPR56 in human glioma U87-MG cells. *Biol Pharm Bull* 38:594–600.
36. Salzman GS, et al. (2016) Structural basis for regulation of GPR56/ADGRG1 by its alternatively spliced extracellular domains. *Neuron* 91:1292–1304.
37. Koide A, Wojcik J, Gilbreth RN, Hoey RJ, Koide S (2012) Teaching an old scaffold new tricks: Monobodies constructed using alternative surfaces of the FN3 scaffold. *J Mol Biol* 415:393–405.
38. Christopoulos A, et al. (2014) International Union of Basic and Clinical Pharmacology. XC. Multisite pharmacology: Recommendations for the nomenclature of receptor allosterism and allosteric ligands. *Pharmacol Rev* 66:918–947.
39. Wilde C, et al. (2016) The constitutive activity of the adhesion GPCR GPR114/ADGRG5 is mediated by its tethered agonist. *FASEB J* 30:666–673.
40. Chiang NY, et al. (2017) GPR56/ADGRG1 activation promotes melanoma cell migration via NTF dissociation and CTF-mediated  $\alpha 12/13$ /RhoA signaling. *J Invest Dermatol* 137:727–736.
41. Prömel S, et al. (2012) The GPS motif is a molecular switch for bimodal activities of adhesion class G protein-coupled receptors. *Cell Rep* 2:321–331.
42. Iguchi T, et al. (2008) Orphan G protein-coupled receptor GPR56 regulates neural progenitor cell migration via a G alpha 12/13 and Rho pathway. *J Biol Chem* 283:14469–14478.
43. Wu MP, et al. (2013) G-protein coupled receptor 56 promotes myoblast fusion through serum response factor- and nuclear factor of activated T-cell-mediated signalling but is not essential for muscle development in vivo. *FEBS J* 280:6097–6113.
44. Kishore A, Hall RA (2017) Disease-associated extracellular loop mutations in the adhesion G protein-coupled receptor G1 (ADGRG1; GPR56) differentially regulate downstream signaling. *J Biol Chem* 292:9711–9720.
45. Wootten D, Christopoulos A, Sexton PM (2013) Emerging paradigms in GPCR allosterism: Implications for drug discovery. *Nat Rev Drug Discov* 12:630–644.
46. Wootten D, Miller LJ, Koole C, Christopoulos A, Sexton PM (2017) Allosterism and biased agonism at class B G protein-coupled receptors. *Chem Rev* 117:111–138.
47. Christopoulos A (2014) Advances in G protein-coupled receptor allosterism: From function to structure. *Mol Pharmacol* 86:463–478.
48. Gingell JJ, et al. (2016) An allosteric role for receptor activity-modifying proteins in defining GPCR pharmacology. *Cell Discov* 2:16012.
49. Christopoulos A, Kenakin T (2002) G protein-coupled receptor allosterism and complexing. *Pharmacol Rev* 54:323–374.
50. Stoveken HM, et al. (2016) Dihydropyridone is a small-molecule selective adhesion G protein-coupled receptor antagonist. *Mol Pharmacol* 90:214–224.
51. Yang TY, et al. (2015) Expression and immunoaffinity purification of recombinant soluble human GPR56 protein for the analysis of GPR56 receptor shedding by ELISA. *Protein Expr Purif* 109:85–92.
52. Sha F, et al. (2013) Dissection of the BCR-ABL signaling network using highly specific antibody inhibitors to the SHP2 SH2 domains. *Proc Natl Acad Sci USA* 110:14924–14929.
53. Oganessian N, Kim R, Kim S-H (2004) On-column chemical refolding of proteins. *Pharmagenomics* 6:177–182.
54. Tsumoto K, et al. (2004) Role of arginine in protein refolding, solubilization, and purification. *Biotechnol Prog* 20:1301–1308.